Wave-induced breakout of untrenched submarine pipes on sand

Echappement dû à ondes de tuyaux sous-marins posés sur sable

X.YGu, F.P.Gao & Q.Pu – *Institute of Mechanics, Chinese Academy of Sciences, Beijing, P.R.China*

ABSTRACT: Wave-induced breakout of the untrenched submarine pipes on sand is investigated experimentally in the U-shape oscillatory flow water tunnel. The instability processes of the pipes in free condition and in condition with constraints against rolling are revealed. Linear relationships between Froude number and non-dimensional pipe weight are obtained. Effects of initial embedment, loading history and particle size are observed. Test results are compared with those conducted under cyclic loading exerted mechanically. The physics of the wave-soil-pipe interaction is clearer than before.

RÉSUMÉ: L'échappement dû à ondes de tuyaux sous-marins posés sur le sable est étudié expérimentalement dans le tunnel d'eau courante en U oscillant. Les processus de l'instabilité de tuyaux sous condition libre et sous condition où l'on contraint le roulement est révélés. Les relations linéaires entre le nombre de Froude et le poid de tuyaux sans dimension sont obtenues. Les influences de l'encastrement initial, l'histoire de chargement et le diamètre des particules sont observées. Les résultsts sont comparés avec ceux obtenus sous le chargement cyclique exercé mécaniquement. La physique de l'interaction des onde-sol-tuyaux est plus clair qu'auparavant.

1 INTRODUCTION

Lateral stability of a marine pipeline requires a balance between the hydrodynamic force, pipeline weight and seabed resistance. If the lateral resistance of pipes on seabed can not offset against the horizontal component of the hydrodynamic force, pipe breakout occurs. Extensive full-scale tests on untrenched pipes on sand under cyclic loading, simulating the loading history of pipelines on the seabed, had been carried out decade of years ago (Brennodden et al. 1986, Palmer et al. 1988). The experiments told the lateral resistance should include a soil passive resistance component besides the Columb friction (Wagner et al. 1987, Brennodden et al. 1989). The result has been applied in the late design standards of submarine pipeline stability (Det norske Veritas 1988, Allen et al. 1989). However, in the above experiments, the simulation of the cyclic loading is generated mechanically. It is different from the wave loading on the seabed in reality. So the physics of the pipe-soil interaction process are not well understood, as stated by Hale et al (1991).

Wave loading as a hydrodynamic force acts on the pipe as well as on the seabed, and the seabed response to the hydrodynamic force will also affect the force on the pipe. Thus the on-bottom stability of submarine pipelines involves the interaction between wave, soil and pipe. The objective of this paper is to reveal the difference of the instability process of untrenched submarine pipeline on sand under hydrodynamic force and that under mechanically exerted cyclic loading.

2 TEST SET UP

2.1 *Test facility*

Under the wave action, the water particles oscillate periodically with certain velocities. For simulating the oscillating movement of water particles in the horizontal direction, tests are conducted in the U-shape oscillatory flow water tunnel, as shown in Figure 1. The water tunnel is made of plexiglass with section area of 0.2 × 0.2 m^2. By using an air blower with a butterfly-valve, the water accomplishes a simple harmonic oscillation:

$$A = A_0 \sin(\omega t) \qquad (1)$$

where $\omega = 2\pi / T$; A_0 = amplitude of the oscillating flow; ω = cyclic frequency; T = period of the oscillating flow, which equals 2.6 sec. The amplitude can be varied continuously within 5-200 mm. Thus the maximum water particle velocity of the oscillating flow U_m is as follows:

$$U_m = \omega A_0 \qquad (2)$$

The water level change is recorded by using a water pressure transducer and data acquisition system. The lower part of the water tunnel constitutes the test section, under which a soil box with length of 0.6 m, width of 0.2 m, depth of 0.035 m is constructed.

During the test the amplitude of the oscillatory flow is controlled to simulate the history of wave loading, and the instability process of the pipe is observed and recorded by the video camera.

2.2 *Test pipes*

The pipes are composed of aluminium, with length of 0.19 m. Pipes of 1.4, 2.0 and 3.0 cm diameter with different weights are used. The pipes are tested in two extreme conditions. One is in free condition, i.e. laid directly on the soil surface with a small initial embedment. Under a certain flow velocity, the pipe will roll. This kind of tests will be denoted by the letter F. Another kind of test pipes, denoted later by C, are constrained against rolling by using an attachment shown in Figure 2. The attachment consists of two parallelograms, which permit the pipe to move horizontally and vertically, but not to roll. The pipe weight is corrected due to the attachment.

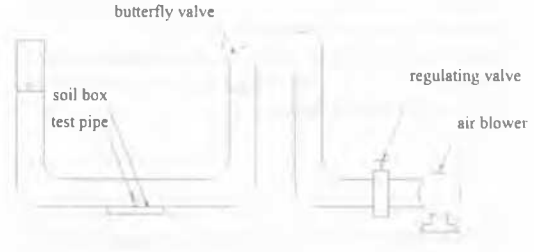

Figure 1. Scheme of the U-shape water tunnel.

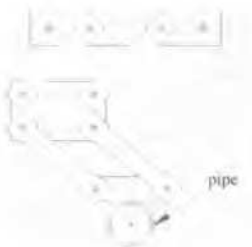

Figure 2. Scheme of attachment for constraining the pipe against rolling.

Owing to the pipe weight and the operation reason, an initial embedment (Z_0/D = 0.03-0.05) always exists.

2.3 *Test soil*

The test sands consist of medium sand and fine sand, the index properties of which are shown in Table 1. The moist sand is first saturated, then packed in the soil box under water, and finally trimmed with a scraper. The difference of the unit weight for one sand in different tests is controlled within the error of 5‰.

Table 1. Index properties of the test sands.

Sand type	Effective particle size	Uniformity coefficient	Relative density	Void ratio	Unit weight	Dry unit weight
					kN / m³	kN / m³
Medium	0.30	1.4	0.73	0.37	19.00	14.80
Fine	0.11	2.0	0.56	0.60	21.05	17.47

3 NON-DIMENSIONAL PARAMETERS

Non-dimensional parameters related to the flow around the pipe are as follows:

Reynolds number Re, the ratio of inertia force to viscous force (Massey 1983):

$$\mathrm{Re} = \frac{U_m D}{\nu} \tag{3}$$

Froude number Fr, the ratio of inertia force to gravity force, which reflects the dynamic similarity of flow with gravity forces acting (Massey 1983), and is an important parameter in case of water-structure-soil interaction (Poorooshasb 1990):

$$Fr = \frac{U_m}{\sqrt{gD}} \tag{4}$$

Keulegan-Carpenter number KC, non-dimensional parameter related to the hydrodynamic force on the pipe under wave action (Herbich 1985):

$$KC = \frac{U_m T}{D} \tag{5}$$

where ν = viscosity; g = gravity acceleration.

Sandy bottom is distributed in many areas in South China Sea, where Fr and KC change between 0-0.5 and 0-20 respectively. In our test condition, Fr and KC are close to these ranges, but Re is smaller than the actual condition for two orders.

Since the study of the wave-soil-pipe interaction directly affects the designed pipe weight, the following non-dimensional parameter of pipe weight is introduced:

$$G = \frac{W_s}{\gamma' D^2} \tag{6}$$

where Ws = submerged weight of pipe per unit length, γ' = buoyant unit weight of soil.

4 EXPERIMENTAL RESULTS

4.1 *Instability process*

When the amplitude of oscillatory flow A_0 increases with a constant velocity, the following phenomena are observed.

At $t = t_s$, within a distance apart from the pipe, the sand grains at the bed surface start to move visibly. Onset of scour occurs. When the water particle velocity is enough to create considerable amount of sediment in suspension, it forms the main contribution to the sediment transport and piles up in the outer directions. While in the vicinity of the pipe, pits are gradually formed on both sides.

For the pipes in free condition, at $t = t_r$, the pipe begins to rock slightly. At $t = t_d$, the pipe detaches itself from the sand bed (see Figure 3a). At $t = t_b$, the pipe suddenly rolls out, or breakout takes place. In most cases in our tests, t_b almost coincides with t_d.

For the pipes in case C, the pipe movement is not observed visibly until $t = t_m > t_d$. Then the vertical and horizontal movements develop gradually, as shown in Figure 4. At $t = t_f$, the horizontal displacement amplitude reaches 0.2 D. This condition is considered as breakout (see Figure 3b).

The instability process of pipes with different submerged weight is shown in Figure 5. The figure shows that the erosion occurs at the same flow velocity for both two kinds of pipes. It implies that the water particle velocity is the main cause of onset of scour or erosion. At that moment the pipe is stable, and the pipe weight has no effect on erosion. Figure 5 also shows that the pipes in case C are much more stable than the pipes in case F. For the pipes with weight $Ws \geq (Ws)_u$, breakout doesn't occur for pipes in case F, and the horizontal displacement is less than 0.2 D for case C.

4.2 *Correlation between pipe weight and hydrodynamic parameters*

Since the real submarine pipeline can not roll, t_b in the free condition is excluded in the data reduction. The water particle velocity at t_d is used for calculating the hydrodynamic parameters. While for case C, the hydrodynamic parameters are calculated from the water particle velocity at t_f.

The correlation between KC number and non-dimensional pipe weight G for medium sand is shown in Figure 6. For the same diameter, exists linear KC-G relationship. For different pipe diameters, linear KC-G relationships are different. It shows that in case of using KC number for data reduction, the effect of pipe diameter is obvious.

Figure 7 shows the correlation between Fr and G for medium sand. All the data with different pipe diameters fall within the same linear relationship. The obtained two lines can be regarded as the critical lines for pipe instability for cases F and C. The upper position of the Fr-G line for case C tells again that these pipes are more stable than those in free condition. In reality, the pipes can not roll, but it is not fully constrained either. Sometimes rocking is possible. So the real critical line for pipe instability should lie between these two lines and nearer the upper line. For $G > G_u$, where $G_u = (W_s)_u / (\gamma' D^2)$, Fr-G line will turn upward.

Since the Froude number in our tests is close to that in real condition, it is convenient to find out the pipe weight for the prototype from the Fr-G correlation.

4.3 *Effect of initial embedment*

Three different values of initial embedment (Z_0/D = 0.05, 0.10, 0.15) have been tested by us with one pipe in free condition. The results are shown in Table 2. For the smallest Z_0/D, breakout occurs just after t_d. The increase of Z_0/D doesn't much affect the oscillating flow amplitude at the beginning of scour A_s, but increases the values of A_r and A_d (flow amplitude at t_r and t_d). For Z_0/D =0.1, although detachment has been observed after the pipe rocking, breakout does't occur due to the piling up of the sediments on both sides of the pipe. For even larger initial

embed- ment, after some time of slightly rocking, self-burial occurs. Thus the on-bottom stability increases with the increase of initial embedment.

Table 2. Results with different initial embedment.

Z_0/D	A_s	A_r	A_d	Does breakout occur?
	cm	cm	cm	
0.05	2.9	4.2	5.0	Yes
0.10	2.9	5.3	5.9	No
0.15	3.0	5.7	Self-burial	No

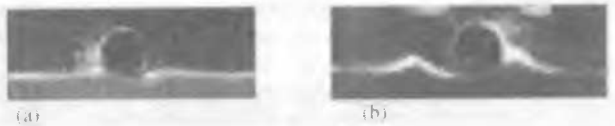

Figure 3. Breakout of the pipe: (a) for case F; (b) for case C.

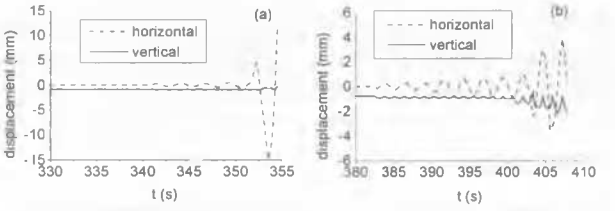

Figure 4. Development of the pipe movements: (a) for case F; (b) for case C.

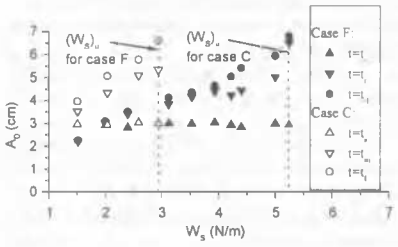

Figure 5. Instability process for pipes with different weight (D=3cm).

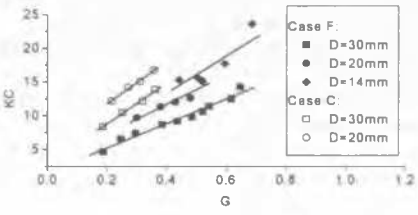

Figure 6. KC-G correlation for medium sand.

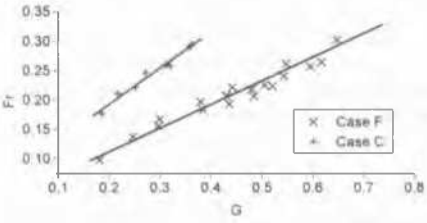

Figure 7 Fr-G correlation for medium sand.

4.4 *Effect of loading history*

In order to explore the effect of loading history, different amplitude velocities have been adopted. The results are shown in Table 3. The velocity of the oscillatory flow amplitude doesn't affect A_s, but A_r and A_d decrease with the increase of flow amplitude velocity dA_0/dt. For the smallest velocity, breakout does not occur.

Table 3. Results with different velocities of flow amplitude.

dA_0/dt	A_s	A_r	A_d	Does breakout occur?
cm/s	cm	cm	cm	
1.8×10^{-2}	2.9	4.1	4.5	Yes
9.0×10^{-3}	2.9	4.2	5.0	Yes
4.5×10^{-3}	2.9	4.5	5.1	No

Furthermore, the storm growing is not always continuous, so experiments with four types of loading history have been undertaken. For type (a), the amplitude increases with a constant velocity as stated above. For the other three types, first increase the flow amplitude with constant velocity till a value of A_c, then maintain A_c for 5 minutes, i.e. about 115 cycles, and finally increase the amplitude as before. The difference of these three types lies in the different values of A_c. For (b), $A_c < A_s$. For (c), $A_s < A_c < A_r$. For (d), A_c is just above A_r. The results are shown in Figure 8. As $A_c < A_s$, since the sand bed has not been disturbed, no effect on pipe stability is observed. When $A_s < A_c < A_r$, the sand grains pile up on both sides of the pipe due to the effect of vortex, thus the pipe stability increases. For the last type (A_c is just above A_r), when A_c is maintained, the slightly rocking pipe returns to the static condition due to the sediment piling. Only after the flow amplitude is increased to some higher level, the pipe slightly rocks again.

It implies that some intermittently growing storm could be beneficial for the pipe stability in spite of the same wave height, and the experimental results with constant amplitude velocity are inclined to the safe side.

4.5 *Effect of particle size*

For sands with different particle size, Fr-G relationships are different (see Figure 9a). Table 1 shows that two test sands are of different relative density and particle size. The relative density has been included in the submerged unit weight, so the additional effect of the particle size should be considered. As we consider medium sand as reference sand and use $G_P = [(d_{10})_M/(d_{10})_T]^{0.2} \times G$ instead of G, where d_{10} is the effective particle size, the suffix M and T denote reference sand and test sand respectively, the linear Fr-G_P relationship for the fine sand coincides with that for medium sand, as shown in Figure 9b.

5 COMPARISION WITH THE PREVIOUS EXPERIMENTS

Wagner et al (1987) reported that cyclic loading caused pipe penetration into the soil and soil mounding in front of the pipe, that resulted in increased lateral soil resistance, which far exceeded those predicted by Coulomb friction. The effect of loading history and initial embedment on the lateral resistance is also indicated (Palmer et al. 1988). Comparing the phenomena from our tests (see Figure 3) and the previous tests (Figure 10), there is some similarity: on both sides of the pipe, soil mounding or piling up of the sediments is investigated. So the same conclusion that the resistance is larger than that predicted by Coulomb friction does exist. Both kinds of the tests also have explored the effect of loading history and initial embedment. The similarity shows that although the previous tests have not included the real hydrodynamic action, the design method based on those tests are correct.

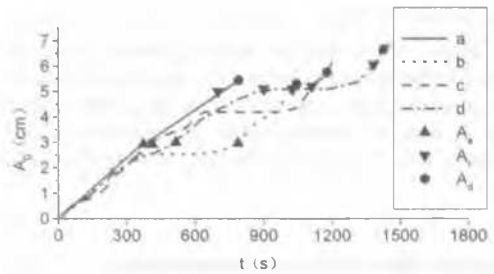

Figure 8. Effect of loading history.

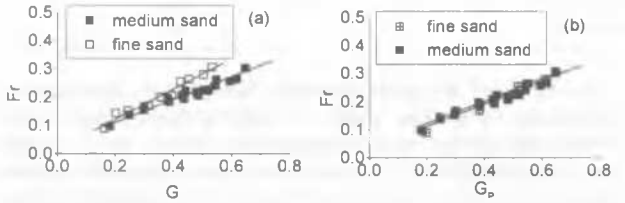

Figure 9. Effect of particle size: (a) Fr-G correlation; (b) Fr-G_P correlation.

Figure 10. Embedment of pipe in soft sediment (from Allen et al, 1989).

However, the mechanism of the phenomena in different kinds of tests is quite different. The previous experimental results are caused by self-penetration of the pipe under cyclic loading exerted mechanically. While in our tests scour or erosion plays an important role, which reflects the actual submarine condition. Scour, as an indication of wave-soil-pipe coupling effect, is a result of combined action of vortexes above the seabed and seepage under the sea bottom (Gu et al, 2001). Thus permeability also serves an important factor, whose affect is included in d_{10}, the diameter for relating particle size and permeability (Lambe & Whitman, 1979).

The pipe-soil interaction models obtained by DNV and AGA are strongly empirical. The parameters in the models strongly depend on how the tests are conducted and the repeatability of the tests. From our wave-soil-pipe interaction tests, the Fr-G or Fr-G_P relationship demonstrates the relationships between water particle velocity, soil properties, pipe diameter and submerged weight of the pipe. All the parameters involved have obvious physical meanings.

Because of the insufficiency of the test data, the final model has not been obtained yet, but the Fr-G relationship implies that it can serve as a supplementary analysis tool for the design.

In order to understand the mechanism thoroughly, measurements of the pipe movements, forces on the pipe, and the pore water pressure beneath the pipe will be conducted further. More extensive and systematic investigations are needed.

6 CONCLUSIONS

1. The wave induced breakout of the untrenched submarine pipe stability on sand is investigated experimentally. Tests are conducted in the U-shape oscillatory flow water tunnel.

2. The instability processes of the pipes in free condition and in condition with constraints against rolling are revealed. The water particle velocity is the main cause for the beginning of the sand particle movements. t_d and t_f are considered as the time for losing stability for the above two conditions.

3. By the non-dimensional analysis the correlations between the pipe weight and hydrodynamic parameters have been obtained. The linear relationships between Froude number and non-dimensional pipe weight can be regarded as the critical lines for pipe instability for two extreme conditions. The real critical line for pipe instability should lie between these two lines and nearer the line for case C.

4. The tests explore that factors, such as initial pipe embedment, loading history and particle size, affect the pipeline stability.

5. Test results between the wave-soil-pipe interaction and pipe-soil interaction under cyclic loading exerted mechanically are compared. The phenomena are similar, but the mechanism is quite different.

6. In order to understand the mechanism thoroughly and to reflect the wave-soil-pipe coupling effect in the practical design, more extensive and systematic investigations are needed.

ACKNOWLEDGEMENT

This study is jointly supported by the Chinese National Scientific Foundation Projects (19772057, 19772065) and the key project of Chinese Academy of Sciences (KZ951-A1-405-01).

REFERENCES

Allen, D.W., Lammert, W.F., Hale, J.R. & Jacobsen, V. 1989. Submarine Pipeline On-Bottom Stability: Recent AGA Research. *OTC paper 6055.*

Brennodden, H., Sveggen, O., Wagner, D.A. & Murff, J.D. 1986. Full-Scale Pipe-Soil Interac tion Tests. *OTC paper 5338.*

Brennodden, H., Lieng, J.T., Sotberg, T. & Verley, R.L.P. 1989. An Energy-Based Pipe-Soil Interaction Model. *OTC paper 6057.*

Det norske Veritas. 1988. On-Bottom Stability Design of Submarine Pipelines, Recommended Practice E305

Gu, X.Y., Gao, F.P. & Pu, Q. 2001. Wave-Soil-Pipe Coupling Effect Upon Submarine Pipeline On-Bottom Stability. *Acta Mechanica Sinica, English Series,* (in press).

Hale, J.R., Lammert, W.F. & Allen, D.W. 1991. Pipeline On-Bottom Stability Calculations: Comparison of Two State-of-the-Art Methods and Pipe-Soil Model Verification. *OTC paper 6761.*

Herbich, J.B. 1985. Hydromechanics of Submarine Pipelines: Design Problems. *Can.J. Civil Engng*, 12: 863~874

Lambe, T.W. & Whitman R.V. 1979. *Soil Mechanics, SI Version.* New York: John Wiley & Sons.

Massey, B.S. 1983. *Mechanics of Fluids, 5th ed.* London: Van Nostrand Reinhold Co.Ltd.

Palmer, A.C., Steenfelt, J.S., Steensen-Bach, J.O. & Jacobsen, V. 1988. Lateral Resistance of Marine Pipelines on Sand. *OTC paper 5853.*

Poorooshasb, F. 1990. On Centrifuge Use for Ocean Research. *Marine Geotechnology* 9: 141-158.

Wagner, D.A., Murff, J.D., Brennodden, H. & Sveggen, O. 1987. Pipe-Soil Interaction Model. *OTC paper 5504.*